



Contents lists available at ScienceDirect

Clinical Nutrition

journal homepage: <http://www.elsevier.com/locate/clnu>

## Original article

# Resveratrol attenuates high-fat diet-induced non-alcoholic steatohepatitis by maintaining gut barrier integrity and inhibiting gut inflammation through regulation of the endocannabinoid system

Mengting Chen, Pengfei Hou, Min Zhou, Qingbo Ren, Xiaolan Wang, Li Huang, Suocheng Hui, Long Yi<sup>\*\*</sup>, Mantian Mi<sup>\*</sup>

Research Center for Nutrition and Food Safety, Chongqing Key Laboratory of Nutrition and Food Safety, Institute of Military Preventive Medicine, Third Military Medical University, Chongqing, 400038, PR China

## ARTICLE INFO

## Article history:

Received 3 February 2019

Accepted 21 May 2019

## Keywords:

Resveratrol

Non-alcoholic steatohepatitis

Gut microbiota

Intestinal barrier

Endocannabinoid receptor

## SUMMARY

**Background & aims:** This study aims to investigate the ameliorative effects of resveratrol (RSV) in a high-fat diet (HFD)-induced non-alcoholic steatohepatitis (NASH) rat model, focusing on the gut endocannabinoid system (ECS), regulated by RSV, in the maintenance of gut barrier integrity and inhibition of gut inflammation.

**Methods and results:** Male Sprague–Dawley (SD) rats were fed HFD with or without RSV for 6 weeks. The HFD caused increase in body weight, liver index, hepatic lipid accumulation, and inflammation, which was inhibited by RSV. RSV also attenuated gut microbial dysbiosis, with an increase in *Akkermansia muciniphila*, *Ruminococcaceae*, and *Lachnospiraceae*, and a decrease in *Desulfovibrio*. Moreover, RSV led to a reduction of metabolic endotoxemia and colon inflammation in HFD-fed rats. This was indicated by a decrease in bacterial invasion and translocation along with up-regulation of the mRNA levels of occludin, ZO1, claudin1, and down-regulation of FAK, MyD88, and IRAK4 in the distal colon. Furthermore, RSV inhibited HFD-induced elevation in the expression of cannabinoid receptor type 1 (CB1) mRNA and suppressed CB2 mRNA levels in the colon. The RSV-induced benefits regarding enhanced gut barrier integrity and reduced intestinal permeability were abrogated with a CB1 agonist, ACEA, whereas the inhibitory effect of RSV on the intestinal inflammation was abolished by a CB2 antagonist, AM630. Moreover, microbiota depletion using a cocktail of antibiotics was sufficient to block RSV-induced reduction in intestinal permeability and gut inflammation, as well as the altered mRNA expressions of CB1 and CB2 in the distal colon.

**Conclusions:** These data indicate that the ECS, particularly the expressions of CB1 and CB2, appears to play a crucial role in the RSV induced anti-NASH effect by maintaining the gut barrier integrity and inhibiting gut inflammation.

© 2019 Elsevier Ltd and European Society for Clinical Nutrition and Metabolism. All rights reserved.

## 1. Introduction

Non-alcoholic fatty liver disease (NAFLD) is one of the most common types of chronic liver disease worldwide [1,2]. As a worse form of NAFLD, non-alcoholic steatohepatitis (NASH) manifests with notable characteristics, including hepatic steatosis, liver inflammation, and advancing fibrosis [1,2]. The pathogenesis of NASH has not been entirely expounded and has been considered as a development from the "two-hit theory" to the "multiple-hit model," involving prevalent multiple parallel factors, including gut–liver axis, inflammatory pathways, and diets [2–4]. The gut–liver axis disorder (involving gut microbiome imbalance, gut–

\* Corresponding author. Research Center for Nutrition and Food Safety, Institute of Military Preventive Medicine, Third Military Medical University, 30th Gaotanyan Main Street, Shapingba District, Chongqing, 400038, PR China. Fax: +86 2368771549.

\*\* Corresponding author. Research Center for Nutrition and Food Safety, Institute of Military Preventive Medicine, Third Military Medical University, 30th Gaotanyan Main Street, Shapingba District, Chongqing, 400038, PR China. Fax: +86 2368771549.

E-mail addresses: [longgyin8341@hotmail.com](mailto:longgyin8341@hotmail.com) (L. Yi), [mi\\_mt2009@hotmail.com](mailto:mi_mt2009@hotmail.com) (M. Mi).

**Abbreviations**

2-AG	2-arachidonoylglycerol
ACEA	arachidonyl-2'-chloroethylamide hydrate
AEA	anandamide
AM630	6-iodopravadoline
A.Muciniphila	Akkermansia Muciniphila
AUC	area under the curve
BCoAT	butyryl-CoA transferase
bw	body weight
CB1	cannabinoid receptor 1
CB2	cannabinoid receptor 2
DAGL	diacylglycerol lipase
ECS	endocannabinoid system
FAAH	fatty acid amide hydrolase
FAK	focal adhesion kinase
FDR	false-discovery rates
FISH	fluorescence <i>in situ</i> hybridization
H&E	hematoxylin and eosin
HFD	high-fat diet
IRAK4	IL-1R-associated kinase 4
KEGG	kyoto encyclopedia of genes and genomes

LC/MS	chromatography-mass spectrometry
LDA	linear discriminant analysis
LeFSe	linear discriminant analysis effect size
LPS	lipopolysaccharide
MAGL	Monoacylglycerol lipase
MyD88	myeloid differentiation primary response 88
NAFLD	non-alcoholic fatty liver disease
NAPE-PLD	N-acylphosphatidyl-ethanolamine-specific phospholipase D
NASH	non-alcoholic steatohepatitis
OGTT	oral glucose tolerance tests
OTUs	Operational taxonomic units
PCA	principal component analysis
PEPCK	phosphoenolpyruvate carboxykinase
PICRUSt	Phylogenetic Investigation of Communities by Reconstruction of Unobserved States
RDA	redundancy analysis
SCFA	short-chain fatty acid
T-CHO	total cholesterol
TG	triglyceride
TLR4	toll-like receptor-4
ZO1	zonula occludens-1

derived lipopolysaccharide (LPS) overgrowth, and alteration of mucosal permeability) was identified to be related to NASH progression [4,5]. Moreover, LPS, derived from some gram-negative bacteria, can access the liver and even the systemic circulation through a dysfunctional intestinal barrier, triggering hepatitis and hepatic impairment [4,6]. LPS regulates the intestinal permeability and inflammation through the toll-like receptor (TLR4) signaling pathway and the activation of focal adhesion kinase (FAK)/myeloid differentiation primary response 88 (MyD88)/IL-1R-associated kinase 4 (IRAK4) signaling pathway [7]. Besides, short-chain fatty acids (SCFA), containing butyrate, propionate, and acetate produced from the microbial degradation products in the gastrointestinal tract, are the critical elements that maintain intestinal barrier integrity [8–10]. At present, no drug has been approved for the treatment of NASH. However, several studies indicate that lifestyle modifications, especially the inclusion of dietary supplements, may improve hepatic steatosis and inflammation [1].

Resveratrol (RSV) is a natural polyphenol present mainly in grapes, berries, and other plants. Several studies suggest that RSV is beneficial for the prevention and cure of multiple metabolic diseases, such as NASH [11,12]. It's well established that RSV is primarily absorbed in the small intestine with high effectiveness. Nevertheless, it has an extremely poor bioavailability as a result of fast metabolism of the human body. Serum levels of free RSV reach their peak concentration within the first 30 min of intake [13–15]. Thereby, the dominant physiochemical benefits of RSV are quite impressive if we compare it to its low bioavailability *in vivo* [16,17]. Recently, researchers have claimed that several polyphenols with low bioavailability probably act principally by reshaping the intestinal microflora [18,19]. It has been discovered that a polyphenol-rich cranberry extract diminished the diet-induced metabolic syndrome in mice in an intestinal microflora-dependent manner [18,19]. Furthermore, previously studies demonstrated that RSV administration could significantly regulate the abundance of specified intestinal bacteria *in vivo* [17,20–22]. Recently, Carta et al. reported that RSV can protect the brain from oxidative stress through the ECS in rat model [23]. The ECS consists of endocannabinoids, cannabinoid receptors, as well as the relevant metabolic enzymes which modulate ligand biosynthesis and

degradation. The ECS is not only comprises of the central nervous system but also the peripheral tissues, especially in liver and gut. Endocannabinoids can modulate the intestinal permeability and inflammation through CB1 and CB2 [9,24]. The intervention of CB1 agonist significantly decreases the expression of intestinal tight junctions, for instance, zonula occludens-1 (ZO1) and occludin [9]. Besides, CB2 is presently estimated to be a promising anti-inflammatory gut biomarker [25]. Thus, we hypothesized that the anti-NASH efficacy of RSV might be a consequence of the maintenance of gut barrier integrity and inhibition of gut inflammation through regulating endocannabinoid system. Our findings uncover a novel role of CB1 and CB2 in the prevention of NASH by dietary RSV supplementation.

## 2. Material and methods

### 2.1. Reagents

RSV (R5010), Arachidonyl-2'-chloroethylamide hydrate (ACEA, Item NO.: A9719), 4000-Da FITC-dextran (46944), ampicillin (171254), metronidazole (M3761), neomycin (N6386) and vancomycin (V2002) were purchased from Sigma–Aldrich. 6-iodopravadoline (AM630, Item NO.: 10006974) was purchased from Cayman Chemical (Michigan, USA).

### 2.2. Animal experiment

The experimental design is shown in [Supplementary Fig. 1](#). Male Sprague–Dawley (SD) rats, weighing 180–220 g, were obtained from the Center of Experimental Animals of the Third Medical University. Animals were maintained under specific pathogen-free (SPF) conditions and housed with free access to sterile food and water. The rats were allowed 1 week to adapt to the laboratory environment, following which they were randomly divided into 4 groups: (1) Normal chow diet (chow) group, which was administered with the chow diet (10% fat, 70% carbohydrate, 20% protein; D12450B, Research Diets); (2) High-fat diet (HFD) group, which was administered with the high-fat diet (45% fat, 35% carbohydrate, 20% protein; D12451, Research Diets); (3) LRSV

group, which was fed HFD accompanied with RSV of 50 mg/kg body weight (bw) per day intragastrically; (4) HRSV group, fed HFD with RSV of 100 mg/kg body weight per day intragastrically. The body weight and food consumption were recorded weekly. Feces and cecal contents were collected at the beginning and the end of the administration. After fasting for 6 h, the oral glucose tolerance tests (OGTT) and gut permeability assays were performed on the rats. After sacrificing them, the samples of blood, liver tissues, as well as distal colon were collected for biomedical analysis. The experiments regarding bacterial translocation, the mRNA expression of tight junction-associated genes, intestinal permeability (4000-Da FITC-dextran, Item No.: 46944; Sigma–Aldrich, 600 mg/kg·bw) [14], and plasma LPS levels (GenScript, Nanjing, China) [9] were performed according to the indicated protocols. For the depletion of gut microbiota test, the rats were subjected to HFD with or without RSV of 100 mg/kg·bw per day for 6 weeks, followed by an administration of broad-spectrum antibiotic (Abx) cocktail solution in water for 4 weeks [9,26]. For the study of the ECS function *in vivo*, the rats were fed HFD with RSV of 100 mg/kg·bw/day for 6 weeks, followed by the administration with or without the CB1 agonist ACEA (1 mg/kg·day), the CB2 antagonist AM630 (1 mg/kg·day), or equal volume of the dissolved solution (vehicle) containing DMSO, cremophor and saline intraperitoneally for an additional 4 weeks [9,27]. The animal procedures were approved by the Animal Ethics Committee of the Third Military Medical University.

### 2.3. Oral glucose tolerance test (OGTT)

OGTT was measured as previously described [10]. The glucose tolerance can be assessed by the area under the curve (AUC).

### 2.4. Histological evaluation

Liver and distal colon sections were submerged in 4% paraformaldehyde. Hematoxylin and eosin (H&E) staining, oil red O staining as well as masson's trichrome staining were performed and assessed in accordance with standard procedures and previous publication [28].

### 2.5. Biochemical parameters

In liver homogenates, the contents of liver triglyceride (TG) and total cholesterol (T-CHO) were measured with enzymatic assay kits (Jiancheng Bioengineering Institute, China). Plasma lipid profiles, such as plasma TG and plasma T-CHO, were quantified using commercial kits (Jiancheng Bioengineering Institute, China). All experiments were tested at least three times.

### 2.6. 16S rRNA gene sequencing

The fecal DNA samples were obtained, amplified, quantified, and sequenced using the Illumina MiSeq platform (Illumina, San Diego, CA, USA). The principal component analysis (PCA), linear discriminant analysis effect size (LEfSe), as well as the redundancy analyses (RDA) were performed with QIIME and R software [9]. The aim of the LEfSe test was to distinguish characteristic microbes among the groups [29]. RDA test was used to find the potential correlations between the bacterial community structure and the environmental factors [30].

### 2.7. Quantitative real-time polymerase chain reaction (qRT-PCR)

Total RNA samples of distal colon and liver sections were obtained by TRIzol reagent method and then reverse transcribed

into cDNA. The qRT-PCR assay was implemented by TB Green™ Premix Ex Taq™ (Takara, Japan). Each sample was conducted at least thrice and normalized to 18s RNA or  $\beta$ -actin by the  $2^{-\Delta\Delta CT}$  method. The primers sequences are stated in [Supplementary Tables 1 and 2](#)

### 2.8. SCFA analysis

SCFA analysis was conducted by Agilent 6890N GC system (Agilent Technologies, PA, USA) as described previously [36] and 2-ethylbutyric acid (Sigma) was treated as an internal reference standard.

### 2.9. Fluorescence in situ hybridization (FISH) with bacteria

The FISH experiment was performed according to the previous work [9]. Universal bacterial probe were synthesized in accordance with previous research shown in [Supplementary Table 3](#).

### 2.10. Liquid chromatography-mass spectrometry (LC/MS) analysis

The content of RSV in plasma and cecum of rats was measured by LC/MS as described previously [17]. Briefly, plasma samples (200  $\mu$ L) were stabilized with 10 mM of ascorbic acid (200  $\mu$ L) and acidified with 200  $\mu$ L of 0.6 M acetic acid. In addition, 300 mg of the cecal content was completely ground in 300  $\mu$ L of physiological saline using a tissue homogenizer (IKA, Germany) for 3 min. The samples were dissolved in 100  $\mu$ L of methanol and 10  $\mu$ L aliquots were submitted for LC/MS analyses.

### 2.11. Statistical analyses

Data analysis was implement with SPSS 13.0 (Chicago, IL). All experimental data are presented as the mean  $\pm$  SEM. Multiple groups were tested by one-way ANOVA followed with Bonferroni multiple comparison tests. A P value < 0.05 was thought to be significant. \*P < 0.05, \*\*P < 0.01, \*\*\*P < 0.001, \*\*\*\*P < 0.0001, ns, no significance.

## 3. Results

### 3.1. RSV attenuates hepatic steatosis and inflammation in rats following HFD

Feeding rats with HFD is an established model for diet-induced NASH, which is accompanied by hepatic steatosis and inflammation [1]. The body weight and liver index (Fig. 1A,B) of rats were increased significantly 6-weeks post HFD feeding, which were notably inhibited by the addition of RSV concentrations of 50 and 100 mg/kg·bw/day compared to the rats fed with HFD alone. Although there were no differences in food intake among the 4 groups (Fig. 1C), HFD clearly increased the hepatic lipid accumulation, hepatocyte hypertrophy, vacuolization, inflammatory cell infiltration, and hepatic fibrosis in rats, compared to that of the chow group, assessed with H&E, oil red O and Masson's trichrome staining each (Fig. 1D-F). Interestingly, the administration of RSV concentration of 50 and 100 mg/kg·bw/day significantly attenuated the HFD-induced hepatic steatosis, inflammation and hepatic fibrosis (Fig. 1D-F). Also, the rats fed with high dose RSV intervention exhibited less hepatic steatosis and fibrosis compared with low dose RSV intervention group. Furthermore, HFD led to significantly raised levels of plasma TG and T-CHO as along with the liver TG and T-CHO compared to those of the chow group (Fig. 1G–J). On the other hand, RSV administration dominantly reversed the HFD-



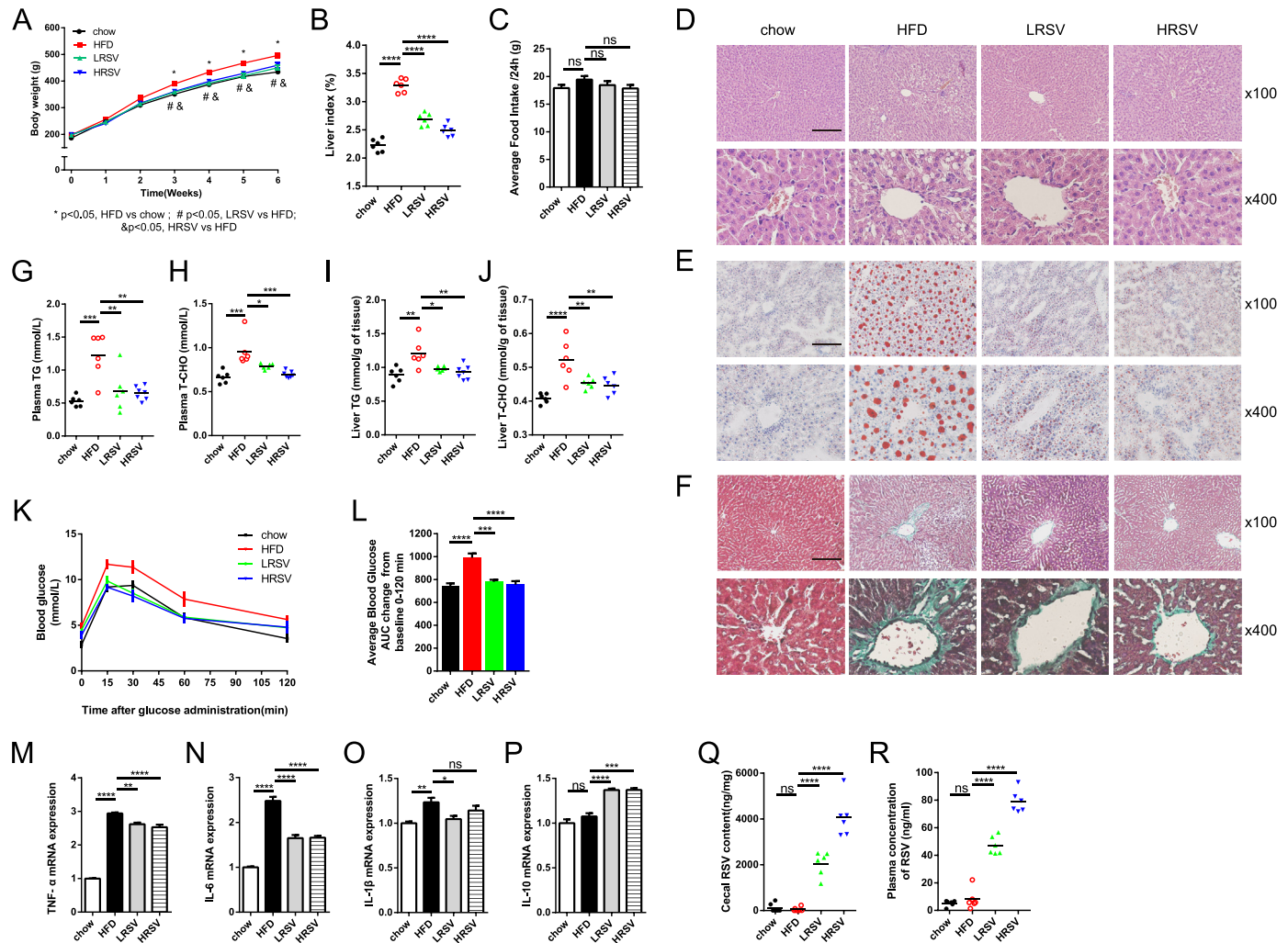


**Fig. 1.** RSV attenuates hepatic steatosis and inflammation in rats following HFD. SD rats were administrated with the normal chow diet (chow) and a high-fat diet (HFD) with or without RSV intragastric administration over 6 weeks. (A) Weight gain curves; (B) Liver index; (C) Food intake; (D–F) Representative photographs of the liver sections with H&E (D), oil red O (E) and Masson's trichrome (F) staining. Scale bar: 200  $\mu$ m;  $\times 100$  magnification (top panel);  $\times 400$  magnification (down panel). (G–J) The plasma TG (G) and T-CHO (H) as well as the liver TG (I) and T-CHO (J) levels were measured with the corresponding assay kits. (K–L) Oral glucose tolerance test (OGTT) (K) in each of the groups and the average change from baseline in the area under the curve (AUC) from 0 to 120 min was calculated (L). (M–P) The mRNA expressions of the inflammatory markers TNF- $\alpha$  (M), IL-6 (N), IL-1 $\beta$  (O), and IL-10 (P) in liver tissues were assessed by qRT-PCR assay. (Q–R) The content of RSV in cecal portion (Q) and plasma (R) were determined by LC/MS assay. The qRT-PCR data were normalized to 18S RNA. Data were presented as the mean  $\pm$  SEM (n = 6). For panel A, \*P < 0.05, HFD vs. chow; #P < 0.05, LRSV/HRSV vs. HFD; for panel B–R, \*P < 0.05, \*\*P < 0.01, \*\*\*P < 0.001, \*\*\*\*P < 0.0001, ns, no significance, compared between the marked groups. Multiple groups were tested by one-way ANOVA followed by Bonferroni's *post hoc* test for all statistical analyses.

induced alteration of plasma and hepatic lipid profiles (Fig. 1G–J). Meanwhile, the blood glucose level was predominantly reduced in the RSV-administered rats compared with HFD alone group (Fig. 1K,L). The expression levels of TNF- $\alpha$ , IL-6, and IL-1 $\beta$  were reduced in the liver tissues of the RSV-fed rats compared to HFD alone feeding group (Fig. 1M–O). Additionally, the expression of IL-10 (Fig. 1P) was remarkably increased in RSV administered groups compared to the HFD group. The RSV contents in cecum and plasma were quite dominant in rats fed with RSV, suggesting its effective absorption by the rats (Fig. 1Q,R). Interestingly, the content of free RSV in plasma was far less than that in the cecum, implying that RSV with a relatively low bioavailability might possibly work via remodeling of the gut microbiota. Taken together, our results suggest that RSV administration can significantly suppress the HFD-induced hepatic lipid accumulation and inflammatory injury in rat models.

### 3.2. RSV remodeled the gut microbial communities in rats following HFD

In total, 973,411 sequences were characterized. The results of rarefaction diversity indicated that most of the variety had been taken (Supplementary Fig. S2A). No significant difference was observed in taxonomic alpha diversity, containing Chao1 index, Abundance-based Coverage Estimator (ACE) and Shannon Index, during the research period (Supplementary Fig. S2 B–D). Subsequent analysis of the intestinal microflora profile revealed that the composition of bacterial community was substantially changed among different samples (Fig. 2A). The PCA analysis, a crucial part of  $\beta$ -diversity indices, illustrated that the bacterial community structure was different apparently among chow, HFD, LRSV and HRSV subgroups (Fig. 2B). The chow group was solitarily located at the top left corner, the LRSV and HRSV clusters stood in the top right corner, while the HFD subgroup was present on the bottom

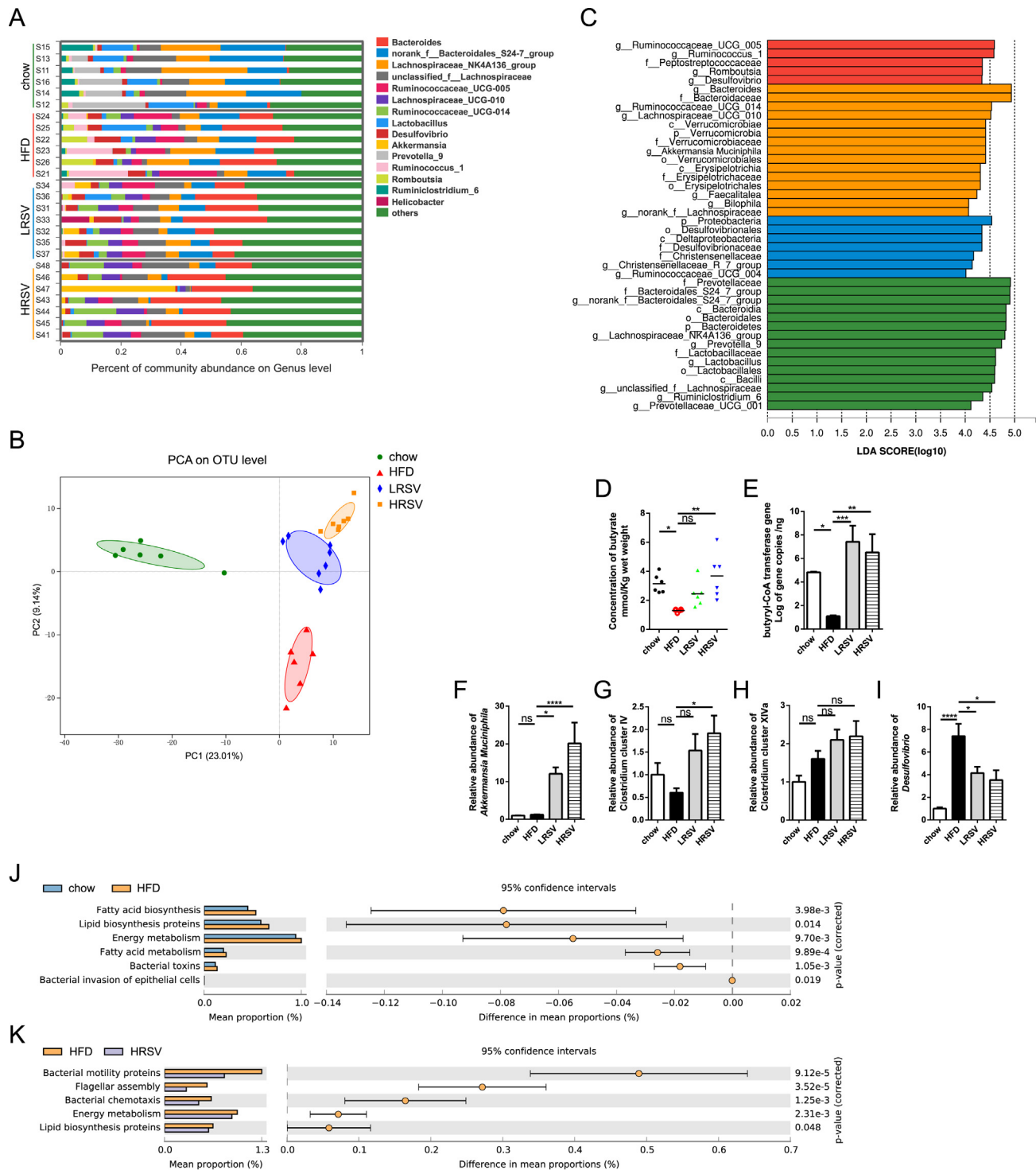


**Fig. 2. RSV remodeled the gut microbial communities in rats following HFD.** (A) Changes of taxonomic composition of gut microbiota at the 6th week. Stacked bar charts showed the individual variability of the relative abundances of major bacterial genus in the study. (B) Unweighted UniFrac PCA analysis of the stool samples using the full set of OTUs at the 6th week. The proportion of the variation can be account for the plotted principal coordinates (PCs) was presented. (C) Linear Discriminant Analysis (LDA) scores derived from LEfSe analysis, showing the biomarker taxa (LDA score >2 and a significance of  $P < 0.05$  determined by the Wilcoxon signed-rank test). (D) The concentration of butyrate in cecal were measured. The abundance of butyryl-CoA transferase (BCoAT) genes (E), relative abundance of *Akkermansia muciniphila* (F), short chain fatty acids (SCFA) producing group *Clostridium* cluster IV (G), *Clostridium* cluster XIVa (H) and *Desulfovibrio* (I) were measured, respectively. (J–K) The function prediction of microbial genes involved in metabolism by PICRUST analysis and based upon Welch's t-test ( $P < 0.05$ ). For panel B, the colorful circles represented 95% confidence intervals calculated by Welch's inverted method. Data were presented as the mean  $\pm$  SEM. \* $P < 0.05$ , \*\* $P < 0.01$ , \*\*\* $P < 0.001$ , \*\*\*\* $P < 0.0001$ , ns, no significance, in comparison with the marked groups. Multiple groups were tested by one-way ANOVA followed by Bonferroni analysis.

right corner (Fig. 2B). Additionally, LEfSe analysis displayed that the LPS-producing bacteria *Desulfovibrio* was increased in the HFD group, while the beneficial bacteria *Akkermansia muciniphila* (*A. muciniphila*), including *Bacteroides*, *Ruminococcaceae*, and *Lachnospiraceae*, responsible for SCFA (e.g. butyrate) production, were elevated at HRSV group (Fig. 2C). Besides, the fecal SCFA test highlighted a striking diminution of butyrate in the rats subjected to 6-week HFD, which was reversed upon administration of 100 mg/kg·bw/day RSV (Fig. 2D). Nevertheless, there was no dissimilarity in the fecal level of acetate and propionate among the 4 groups (Supplementary Figs. S3A and B). In order to analyze the functions of RSV on the SCFA-producing bacteria, we measured butyryl-CoA transferase (BCoAT) genes with qRT-PCR assay. Notably, the gene copies were higher in RSV-fed rats compared to HFD-alone fed rats (Fig. 2E). Meanwhile, the relative abundance of *A. muciniphila* (Fig. 2F), SCFA-producing bacteria (e.g. *Clostridium* cluster IV) (Fig. 2G) and LPS-producing *Desulfovibrio* (Fig. 2I) were significantly reversed in RSV-fed groups, measured by qRT-PCR assays. No difference was observed in the relative abundance of *Clostridium* cluster IV (Fig. 2H). In particular, the HRSV group demonstrated an obvious increase in the relative abundance of *A. muciniphila* and butyrate-producing bacteria with respect to the low-dose of RSV intervention. Butyrate, which is produced principally by *Ruminococcaceae* and *Lachnospiraceae*, could prevent metabolic endotoxemia by strengthening the gut barrier [9,31]. To further evaluate the functional changes associated with the composition of intestinal flora among 4 groups, we used PICRUSt (Phylogenetic Investigation of Communities by Reconstruction of Unobserved States) software package for predicting the relative abundance profiles of KEGG reference pathways. The “fatty acid biosynthesis”, “lipid biosynthesis proteins”, and “bacterial toxins” pathways were significantly raised in HFD group compared to the chow group (Fig. 2J). On the other hand, the biomarkers with “bacterial motility proteins”, “bacterial chemotaxis” and “lipid biosynthesis proteins” pathways were significantly down-regulated in the HRSV group compared to the HFD group (Fig. 2K), demonstrating a vital role of RSV in the blockage of bacterial motility and lipid biosynthesis upon HFD feeding. Above data reveals that RSV reshapes the intestinal microbiota in the HFD-fed rats, which may be conducive to the increased SCFA and decreased LPS production, thereby inhibiting the LPS translocation.

### 3.3. Resveratrol ameliorates the intestinal barrier dysfunction and inflammation in rats following HFD

The intestinal barrier integrity is intimately involved in hepatic steatosis and inflammation through the “gut–liver axis”. To reveal whether RSV could further ameliorate the intestinal barrier integrity and inflammation, we tested the bacterial translocation markers, metabolic endotoxemia, and the mRNA expressions of the associated genes in the distal rat colon. As shown in Fig. 3, the bacterial invasion into the colon intestinal epithelium surface was observed using a universally used fluorescence probe by FISH assay. As expected, RSV administration noticeably protected the intestinal epithelium from the invading bacteria compared to the HFD alone group (Fig. 3A). Furthermore, the plasma levels of bacterial DNA were determined using qRT-PCR assay. In consistency with the FISH results, the bacterial 16S rRNA load in the blood samples was significantly lower in RSV-administered rats relative to the HFD-alone fed rat group (Fig. 3B). Coherently, we also found a significantly decreased intestinal permeability (Fig. 3C) and reduced plasma LPS levels (Fig. 3D) in rats with RSV administration compared to HFD feeding alone. In addition, RSV-fed rats showed up-regulated mRNA levels of occludin (Fig. 3E), ZO1 (Fig. 3F), and Claudin1 (Fig. 3G) in the distal colon, indicating an increased

intestinal mucosal integrity aided by RSV administration (Fig. 3H). As we had speculated, HRSV group exhibited a more obviously ameliorated intestinal barrier integrity compared with the LRSV intervention group. Moreover, the HFD feeding-induced increased pro-inflammatory markers including TNF- $\alpha$ , IL-1 $\beta$ , IL-6, and reduced anti-inflammatory cytokine IL-10 in the rat distal colons, while above conditions were restored by RSV administration (Fig. 3H, I–L). Next, RSV administration significantly reduced the relative mRNA expressions of FAK (Fig. 3M), MyD88 (Fig. 3N), and IRAK4 (Fig. 3O) in the distal colon tissue compared to HFD fed group, involved in the LPS/TLR4 downstream signaling pathway. Cumulatively, these results demonstrate that RSV improves the HFD-induced intestinal barrier dysfunction, leading to a reduction of bacterial invasion and translocation, further suppressing the metabolic endotoxemia and colon inflammation in rats.

### 3.4. RSV maintains the intestinal barrier integrity through CB1 in rats following HFD

It has been demonstrated that ECS activity could be up-regulated or down-regulated by particular microbes (e.g. *A. muciniphila*) [24]. So we quantified the mRNA expressions of CB1 and CB2, as well as ECS-associated metabolic enzymes. HFD feeding resulted in a raised CB1 (Fig. 4A) and decreased CB2 (Fig. 4B) transcript levels in the rats' distal colons. However, the altered mRNA expressions of CB1 and CB2 by HFD feeding were restored by RSV administration. The AEA and 2-AG are the most highly studied ligands for ECS as of now. AEA exhibits higher affinity for CB1 over CB2 receptors, and 2-AG binds to CB1 and CB2 with similar affinities. CB1 and CB2 are highly expressed on enteric nerves and throughout the intestinal mucosa on enteroendocrine cells (CB1), immune cells (CB1 and CB2), and enterocytes (CB1 and CB2). Under physiological conditions, the actions of ECS in the gastrointestinal tract are largely mediated by CB1 [32]. Previous studies showed that AEA increases gut permeability in obese mice through a CB1-dependent mechanism, whereas 2-AG reduces the metabolic endotoxemia and systemic inflammation in a colitis model [32,33]. However, although both of the *in vivo* and *in vitro* data consistently indicated that AEA contributes to the disruption of gut-barrier function (that is, functions as a “gate opener”), while 2-AG seems to be mostly associated with a beneficial effect on gut-barrier function *in vivo* and can be considered as a “gate keeper” [32]. AEA acts as a “gate opener”, and is synthesized by the regulation of N-acylphosphatidyl-ethanolamine-specific phospholipase D (NAPE-PLD) [24,32] while 2-AG, the “gate keeper” is mainly activates CB2 in the gastrointestinal tract, are made from cell membrane phospholipids upon activation of diacylglycerol lipase (DAGL), encoded by DAGL $\alpha$  [24,32,33]. The monoacylglycerol lipase (MAGL) is considered to be the principal 2-AG degrading enzyme, while the fatty acid amide hydrolase (FAAH) is the primary enzyme attributing to AEA degradation [24]. In addition, we found that the RSV-fed rats showed not only decreased mRNA expressions of DAGL $\alpha$  (Fig. 4C) and FAAH (Fig. 4D), but also increased mRNA expressions of MAGL (Fig. 4E) and NAPE-PLD (Fig. 4F) in response to HFD feeding. These results implied that RSV administration might resulted in higher 2-AG concentration and lowered AEA concentration in the distal colon of HFD fed rats. Moreover, the result of Pearson's correlation analysis displayed that *A. muciniphila* and *Lachnospiraceae\_UCG-010* were significantly related to the expression of distal colon occludin by false-discovery rates (FDR) adjustment (Supplementary Fig. S4A). Besides, *Desulfovibrio* was significantly positively correlated with the intestinal permeability, plasma LPS, and the expression of distal colon CB1 (Supplementary Fig. S4A). Consequently, our results demonstrated that RSV



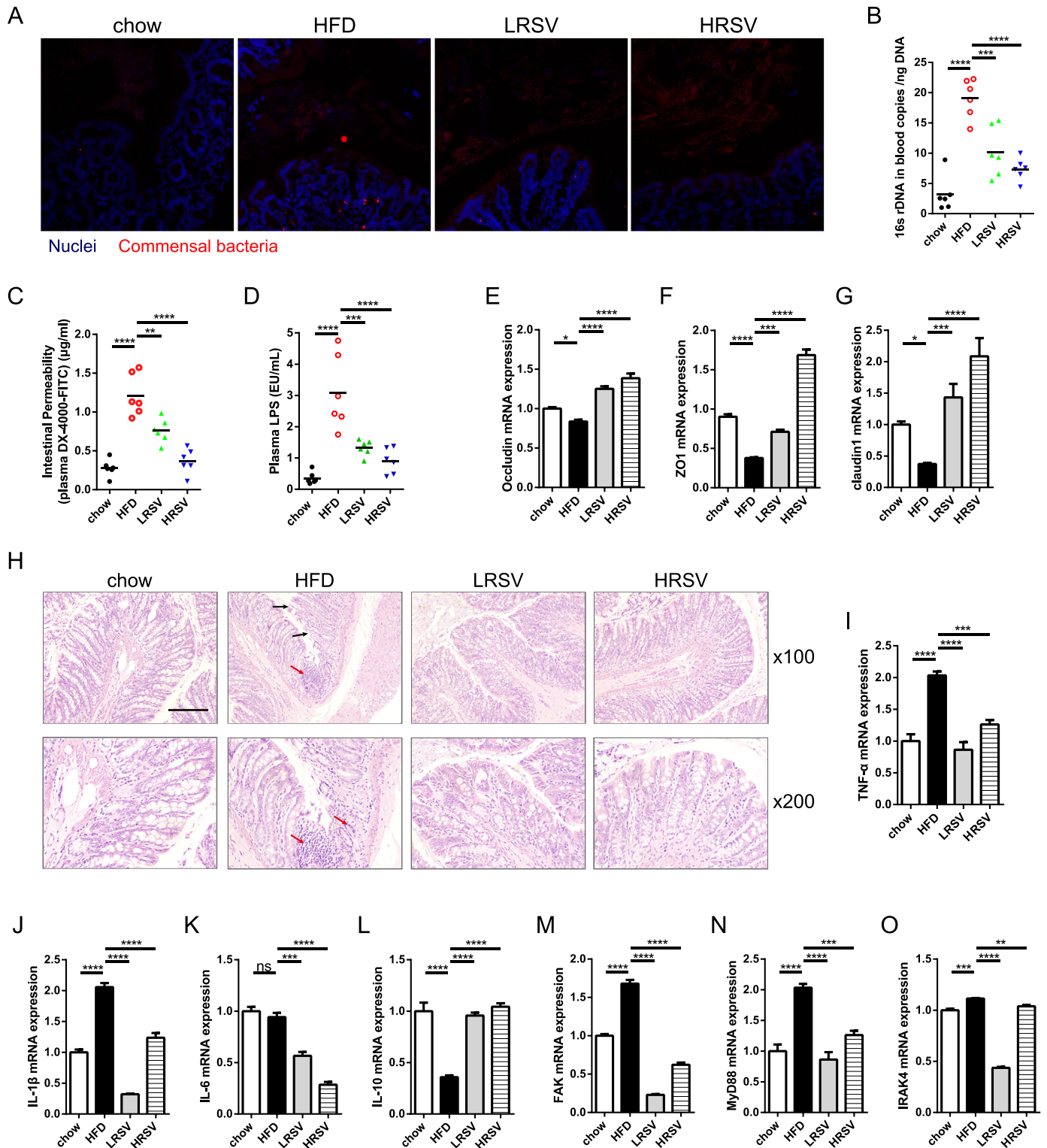


**Fig. 3.** RSV ameliorates intestinal barrier dysfunction and inflammation in rats following HFD. (A) Bacterial invasion in to colonic mucosa visualized by FISH (16S rRNA genes of all bacteria (red) and nuclei (blue)). (B) Total bacterial DNA load (universal 16S rRNA gene copies) in whole blood samples. (C) The intestinal permeability was measured by oral administration with a 4000-Da FITC-dextran. (D) The plasma LPS levels were measured by the corresponding assay kit. (E–G) The relative mRNA expressions of occludin (E), ZO1 (F), and claudin1 (G) in distal colon tissues were assessed by the qRT-PCR assay. (H) Representative photographs of the distal colon sections with H&E staining. Scale bar: 200  $\mu$ m,  $\times$ 100 magnification (top panel);  $\times$ 200 magnification (down panel); Red arrow indicates inflammatory infiltration; Black arrow indicates intestinal epithelial barrier disruption. (I–L) The mRNA expressions of TNF- $\alpha$  (I), IL-1 $\beta$  (J), IL-6 (K), and IL-10 (L) in distal colon tissues were assessed by the qRT-PCR assay. The relative mRNA expressions of LPS/TLR4 downstream signaling pathways FAK (M), MyD88 (N), and IRAK4 (O) in distal colon tissues were assessed by the qRT-PCR assay. Data were presented as the mean  $\pm$  SEM. \* $P$  < 0.05, \*\* $P$  < 0.01, \*\*\* $P$  < 0.001, \*\*\*\* $P$  < 0.0001, ns, no significance. Multiple groups were tested by one-way ANOVA followed by Bonferroni's *post hoc* test.

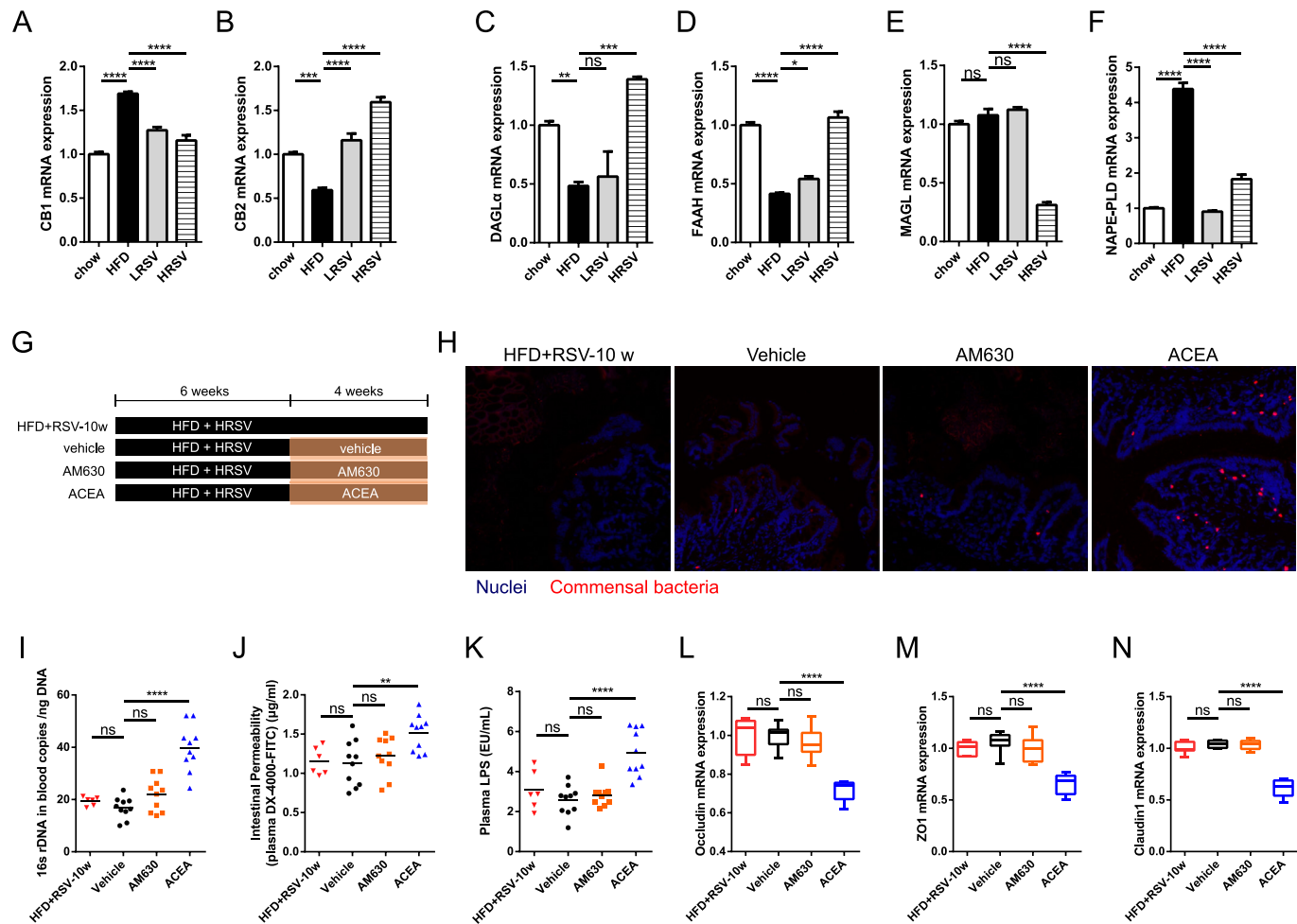


**Fig. 4. RSV maintains the intestinal barrier integrity through CB1 in rats following HFD.** The relative mRNA expressions of CB1 (A), CB2 (B), ECS metabolic enzymes DAGL $\alpha$  (C), FAAH (D), MAGL (E), and NAPE-PLD (F) in distal colon tissues were assessed by the qRT-PCR assay. (G) Schema showing the animal groups and treatments. Male SD rats were fed HFD + HRSV for 6 weeks. Then, HFD + HRSV mice were divided into four groups (HFD + RSV-10w, vehicle, AM630 and ACEA). The rats were intraperitoneally injected with ACEA/AM630/vehicle/no injection for 4 weeks. (H) Bacterial invasion in the colonic mucosa was visualized by FISH (16S rRNA genes of all bacteria (red) and nuclei (blue)). (I) total bacterial DNA load (universal 16S rRNA gene copies) in whole blood samples. (J) The gut permeability to FITC-dextran. (K) The plasma LPS levels were measured by the corresponding assay kit. (L–N) The relative mRNA expressions of occludin (L), ZO1 (M), and claudin 1 (N) in distal colon tissues were assessed by the qRT-PCR assay. Data were presented as the mean  $\pm$  SEM. \* $P < 0.05$ , \*\* $P < 0.01$ , \*\*\* $P < 0.001$ , \*\*\*\* $P < 0.0001$ , ns, no significance. Multiple groups were tested by one-way ANOVA followed by Bonferroni's *post hoc* test.

maintains the intestinal barrier integrity through the regulation of ECS in the distal colon of HFD-fed rats.

We had hypothesized that CB1 and CB2 might be responsible for the advantageous effect of RSV on the maintenance of the intestinal barrier and inhibition of gut inflammation through microflora interaction. To test this hypothesis, rats were fed with HFD and RSV for 4 weeks with or without a CB1 agonist (ACEA), or a CB2 antagonist (AM630), or an equal volume of the dissolved solution (vehicle) (Fig. 4G). As expected, the benefits resulting from RSV feeding in terms of reduced bacterial translocation into mucosal membrane (Fig. 4H) and the peripheral blood (Fig. 4I), the intestinal permeability (Fig. 4J) and plasma LPS level (Fig. 4K) were abrogated with ACEA. Also, the effect of RSV administration on the mRNA levels of intestinal tight junction genes occludin (Fig. 4L), ZO1 (Fig. 4M), and claudin1 (Fig. 4N) along with the butyrate concentration in the cecum (Supplementary Fig. S5A) was eliminated by ACEA. There was no difference in the content of fecal acetate and propionate among the 4 groups (Supplementary Fig. S5 B and C). The results indicate that CB1

chiefly played a beneficial role in the RSV induced gut barrier maintenance in rats following HFD.

### 3.5. RSV inhibits the intestinal inflammation through CB2 in rats following HFD

The ECS, especially the CB2 in the gastrointestinal tract, connects the intestinal microflora with metabolic endotoxemia and intestinal inflammation. It was perceived that the distal colon of the rats with AM630 intervention manifested higher inflammatory infiltration than the other groups (Fig. 5A). What's more, RSV administration induced a decrease in the inflammatory factors TNF- $\alpha$ , IL-1 $\beta$ , and IL-6 in the distal colon, which were inhibited by the addition of AM630 in rats compared to the vehicle group (Fig. 5B–D). No difference was observed in the mRNA expression of IL-10 in the distal colon among the different groups (Fig. 5E). However, the effect of RSV on the mRNA expressions of LPS/TLR4 downstream signaling molecules FAK (Fig. 5F), MyD88 (Fig. 5G) and IRAK4 (Fig. 5H) were abrogated with ACEA rather than AM630.



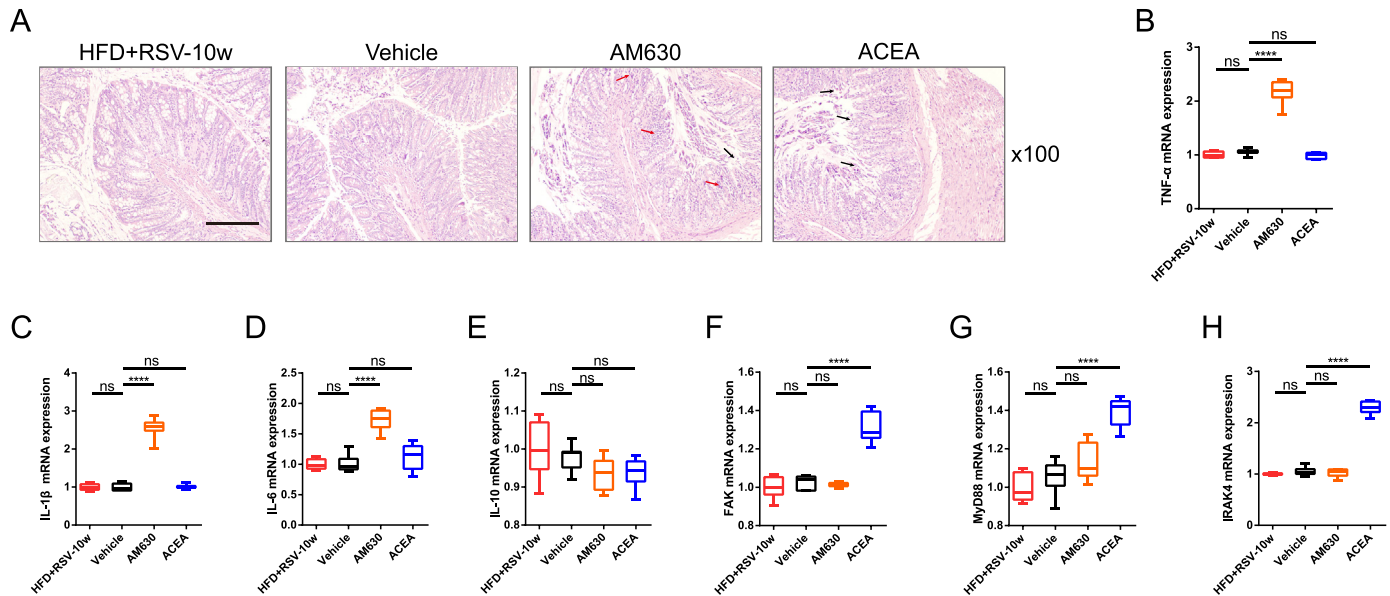


**Fig. 5.** RSV inhibits the intestinal inflammation through CB2 in rats following HFD. (A) Representative photographs of the distal colon sections with H&E staining. Scale bar: 200  $\mu$ m,  $\times 100$  magnification; Red arrow indicates inflammatory infiltration; black arrow indicates intestinal epithelial barrier disruption. (B–E) The mRNA expressions of TNF- $\alpha$  (B), IL-1 $\beta$  (C), IL-6 (D), and IL-10 (E) in distal colon tissues were assessed by the qRT-PCR assay. The relative mRNA expressions of LPS/TLR4 downstream signaling pathways FAK (F), MyD88 (G), and IRAK4 (H) in distal colon tissues were assessed by the qRT-PCR assay. Data were presented as the mean  $\pm$  SEM. \* $P < 0.05$ , \*\* $P < 0.01$ , \*\*\* $P < 0.001$ , \*\*\*\* $P < 0.0001$ , ns, no significance. Multiple groups were tested by one-way ANOVA followed by Bonferroni's *post hoc* test.

Taken together, these results suggested that RSV inhibits the intestinal inflammation through CB2.

### 3.6. RSV ameliorates the intestinal barrier integrity and inhibits gut inflammation associated with the intestinal microbiota

CB1 and CB2 are involved in the maintenance of intestinal barrier integrity. We investigated whether intestinal microbiota is an essential condition for the modulation of CB1 and CB2 in rats by RSV administration using antibiotic treatment. SD rats were fed HFD with or without RSV supplementation for 6 weeks, followed by an antibiotics cocktail to establish the macroscopically germ-free rats [9] (Fig. 6A). Interestingly, markers of metabolic endotoxemia (Fig. 6B and C), body weight (Fig. 6D), concentrations of plasma TG and T-CHO (Fig. 6E,F) and distal colon inflammation state (Fig. 6G–J) were much lower in HFD + RSV rats than in the HFD group, and these effects were markedly reversed upon Abx administration. Our results suggested that the intestinal microbiota primarily mediates the advantageous impact of RSV on intestinal barrier integrity and symptoms of NASH. Besides, the Abx induced microbiota depletion causing RSV-induced suppression of CB1 expression and activation of CB2 in distal colon tissue was significantly abolished (Fig. 6K,L). Ultimately, our findings inferred that the supportive impact of RSV on regulation of the CB1 and CB2 expression in distal colon was associated with the gut microbiota.

### 3.7. There were significant correlations among samples, microbial species, and physiological biochemistry factors by redundancy analysis (RDA)

To find the potential correlations among samples, the bacterial community structures, and the physiological biochemistry factors, RDA test was conducted based on the characteristic bacterial 16S rRNA gene sequences and the measured physiological biochemistry parameters (Fig. 7). The correlations among the above data were represented by the length and angle of the arrows. The length of the

physiological biochemistry factors arrows can represent the influence of corresponding factors on bacteria data; the angle formed between the arrows shows the positive or negative correlation (Acute angle, positive correlation; Obtuse angle, negative correlation; Right angle, no correlation). *Desulfovibrio* manifested a significantly positive correlation with intestinal permeability, in addition to plasma LPS and colon CB1 mRNA expression. The characteristic bacteria, including *A. muciniphila*, *Ruminococcaceae*, and *Lachnospiraceae*, demonstrated a significantly positive correlation with the cecal concentration of butyrate as well as the mRNA expressions of ZO1, occludin, and CB2 in the distal colon.

## 4. Discussion

NASH is a multifactor liver disease [1]. The "multiple-hit" hypothesis had emphasized that the "gut-liver axis", including the gut microbiota and gut barrier integrity, served as crucial element in the pathogenesis of NASH [4]. The impaired gut barrier integrity and metabolic endotoxemia originating from gut microbial dysbiosis are responsible for the development of NASH [2,4,5,32]. A newfangled and safer treatment is urgently required for controlling the progression of NASH. In this study, we found that the RSV was effective in prevention of NASH in HFD-induced rats. Besides, the anti-NASH effect of RSV resulted from the reduced intestinal permeability and gut inflammation, which might be mediated through ECS modulation, particularly the expressions of CB1 and CB2 in distal colon of rats (Fig. 8). Treatment with CB1 agonist eliminates the beneficial effect of RSV (maintaining the gut barrier integrity), while the addition of CB2 antagonist abolished the inhibitory effect of RSV on the intestinal inflammation. Thus, this is the first report stating that RSV might exert the anti-NASH benefits through the ECS, providing a novel therapeutic approach towards managing the gut barrier strength of NASH patients.

Despite of its low-level bioavailability, RSV displays high-efficiency biological benefits *in vivo* [16,17]. However, there is a contradiction between the low bioavailability of RSV and its high

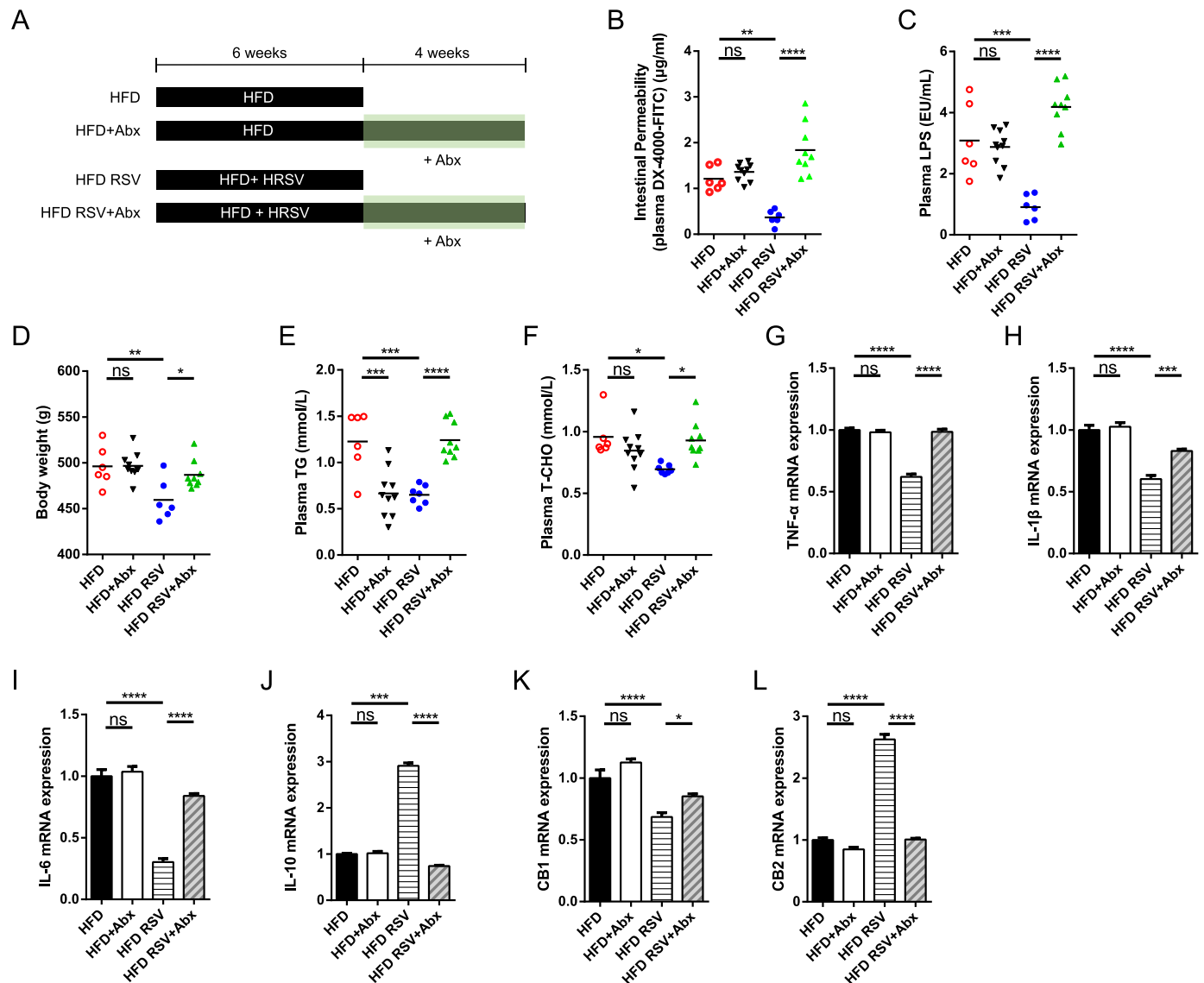


**Fig. 6. RSV ameliorates the intestinal barrier integrity and inhibits gut inflammation associated with the intestinal microbiota.** Male SD rats received HFD, or HFD + HRSV for 6 weeks and were then treated with a broad spectrum antibiotic cocktail (Abx) consisting of ampicillin, vancomycin, neomycin sulfate and metronidazole for 4 weeks to induce microbiota depletion. Blood and tissue samples were subjected to various analyses and data were analyzed before and after Abx supplementation. (A) Schema showing the animal groups and treatments. The intestinal permeability (B), plasma LPS levels (C), and body weight (D) were measured. Plasma TG (E) and T-CHO (F) were measured with the corresponding assay kits. The mRNA expression levels of TNF-α (G), IL-1β (H), IL-6 (I), and IL-10 (J) in distal colon tissues were assessed by the qRT-PCR assay. The mRNA expression levels of CB1 (K) and CB2 (L) in distal colon tissues were assessed by the qRT-PCR assay. Data were presented as the mean ± SEM. \*P < 0.05, \*\*P < 0.01, \*\*\*P < 0.001, \*\*\*\*P < 0.0001, ns, no significance. Multiple groups were tested by one-way ANOVA followed by Bonferroni's *post hoc* test.

efficacy. In this study, we found that the content of the free RSV in cecum was far more than that in the plasma. Thus, it's quite possible that RSV exerts an important role in the intestinal tract. However, the mechanisms that underlie these functions of RSV in intestine remain obscure. Recently, several evidences which were consistent with our experimental results sustained the conception that RSV with poor bioavailability may be performing principally by reshaping the intestinal microflora [17]. We also discovered that RSV could regulate the gut microbiota community structure. Importantly, our findings revealed that RSV inhibited HFD-induced increased CB1 mRNA and decreased CB2 mRNA levels in the colon, implying that CB1 and CB2 regulation was a part of the *in vivo* benefits of RSV. However, it's still not clear how RSV regulates the CB1 and CB2 expression in rats. It has been demonstrated that ECS activity could be up-regulated or down-regulated by particular

microbes via regulation of ECS ligands (for example *A. muciniphila*) [24]. Reports also suggest that the HFD-fed mice were intragastrically administrated with *A. muciniphila*, while increasing the concentration of 2-AG, 2-oleoylglycerol (2-OG), and 2-palmitoylglycerol (2-PG) in the ileum [34]. Thus the administration of *A. muciniphila* was conducive to maintaining the intestinal barrier integrity and inhibiting gut inflammation [34]. In our study, dietary RSV could directly up-regulate the abundance of *A. muciniphila* and resulted in the altered expressions of CB1 and CB2, apart from the ECS-associated metabolic enzymes in the distal colon of HFD-fed rats. Thus, we hypothesized that the decreased CB1 and increased CB2 mRNA expressions induced by RSV might be accompanied with the alteration of 2-AG and AEA in the distal colon, which might be associated with the increased abundance of *A. muciniphila* induced by RSV. AEA acting as "gate opener", and

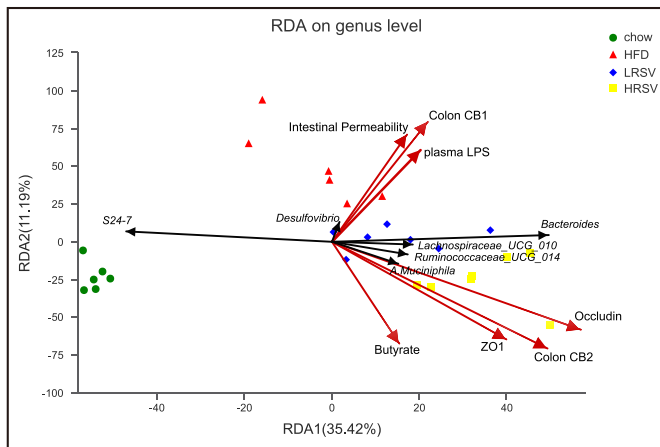


**Fig. 7. Redundancy analysis (RDA) diagram showing the correlations among samples, microbial species, and physiological/biochemistry factors.** Characteristic bacteria (black arrows), samples (symbols) and physiological/biochemistry factors (red arrows) are shown in the diagram. The values of axes 1 and 2 are the percentages explained by the corresponding axis. Labels implicate all four clusters. Names of the parameters were drawn as vectors by their association to the first two components.

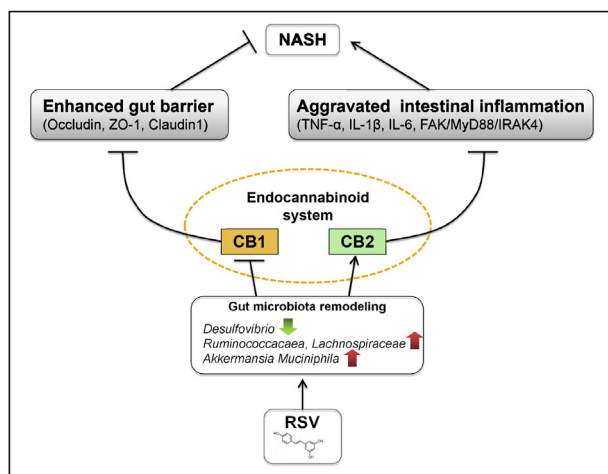


**Fig. 8. Illustration of the anti-NASH effect of RSV through ECS.** The gut microbial remodeling (such as decreased Gram-negative LPS-producing bacteria e.g. *Desulfovibrio*, increased beneficial bacteria e.g. *Akkermansia muciniphila*, and increased butyrate-producing bacteria e.g. *Ruminococcaceae* and *Lachnospiraceae*) enhanced the gut barrier integrity and decreased metabolic endotoxemia, which were responsible for the progression of NASH. RSV administration ameliorates NASH by remodeling the gut microbiota and then regulating the ECS, particularly the expressions of CB1 and CB2 in the colon of rats, leading to the enhanced intestinal barrier integrity and the reduced intestinal inflammation.

2-AG, as a “gate keeper”, mainly activated CB2 in the gastrointestinal tract. Hence, we inferred that RSV may increase the mRNA expression of CB2 in distal colon of rats, which can hinder the intestinal inflammation. In addition, RSV administration maintained the gut barrier integrity and decreased the mRNA expressions of CB1 in the distal colon of rats. RSV-induced benefits in terms of the increased gut barrier integrity and reduced intestinal permeability were abrogated with a CB1 agonist ACEA, whereas the inhibitory effect of RSV on the intestinal inflammation was abolished by a CB2 antagonist AM630.

Our research also established that RSV administration increased the number of butyrate-producing *Clostridium* clusters

IV (e.g. *Ruminococcaceae* and *Lachnospiraceae* in diet-induced NAFLD rats. Previous studies had emphasized that butyrate can ameliorate the function of gut barrier (such as increasing the expressions of occludin and ZO1), while offering essential energy source to the enterocytes, resulting in inhibition of LPS translocation [8,9,31,35]. Besides, butyrate depresses the level of proinflammatory cytokines, up-regulates anti-inflammatory IL-10 expression and activates Treg cells, resulting in blocking the progression of colitis [36]. It's well-known that butyrate diminishes HFD-induced steatohepatitis through remodeling intestinal microbiota community structure and enhancing gut barrier integrity, thereby preventing LPS from translocating through this barrier [31,36]. Our results demonstrated that cecal butyrate had a positive correlation with the relative abundance of *Ruminococcaceae\_UCG\_014* and *Lachnospiraceae\_UCG\_010* (Fig. 7) in RSV administration groups, entailing the beneficial effect of RSV on increasing the butyrate-producing bacteria as well as enhancing the butyrate concentration. The data from our antibiotics-induced depletion of microbiota support the notion that the impact of RSV on enhancing gut barrier and its anti-inflammatory effect may be attributed to gut microbiota in rats. The antibiotics, CB1 agonist, and CB2 antagonist involving experiments implied that the beneficial regulation of dietary RSV on the CB1 and CB2 expression in distal colon mainly mediated through the regulation of intestinal microbiota. In addition, the results displayed that RSV intervention reduced the abundance of genes concerning “bacterial motility proteins”, “flagellar assembly” and “lipid biosynthesis proteins” on the basis of the function prediction through the PIC-RUST analysis [37]. Above results can be principally attributed to the decrease in *Desulfovibrio* upon RSV treatment as it was the fundamental bacterium that mainly contributed to HFD feeding rats (Fig. 2C and I). Gut-derived LPS induced enhancement in gut permeability and intestinal inflammatory conditions were modulated by TLR4-dependent stimulation of the FAK/MyD88/IRAK4 signaling pathway [7].

## 5. Conclusion

Our results collectively indicate that the ECS, particularly the expressions of CB1 and CB2, appears to play a crucial role in the anti-NASH effect of RSV by the maintenance of gut barrier integrity and inhibition of gut inflammation. Our research also implied that RSV attenuates high-fat diet induced gut barrier impairment by inhibiting colonic CB1, and abrogates the aggravated intestinal inflammation via activating CB2, resulting in LPS translocation suppression (Fig. 8). Ultimately, considering the fact that ECS imbalance, intestinal microbial dysbiosis, impaired intestinal barrier, as well as aggravated intestinal inflammation are frequently associated with chronic liver diseases, the effect of RSV on alleviating these conditions emphasizes the potential of RSV supplementation as a therapeutic strategy for preventing NASH.

## Author contributions

M.C. initiated the project, designed and performed experiments, analysed the data and drafted the manuscript; M.C., Q.R., S.H., L.H., P.H., and M.Z., collected samples and performed the experiments. L.Y. contributed to technical support and data interpretation. M.M. and L.Y. designed the project, obtained funding, helped with the writing of the paper, and finalized the manuscript. All authors read and approved the final manuscript. None of the authors reported a conflict of interest.



## Data availability

The sequences reported in this paper have been deposited in the NCBI database (accession number PRJNA507704).

## Funding sources

This research was supported by the research grants from National Natural Science Foundation of China (81872625 and 81470562) and Natural Science Foundation of Chongqing, China (cstc2018jcyjAX0124).

## Conflicts of interest

All authors declare no conflict of interest.

## Acknowledgments

Gut microbiome sequencing analysis were performed using the free online platform of Majorbio I-Sanger Cloud Platform ([www.i-sanger.com](http://www.i-sanger.com)).

## Appendix A. Supplementary data

Supplementary data to this article can be found online at <https://doi.org/10.1016/j.clnu.2019.05.020>.

## References

- [1] Younossi Z, Tacke F, Arrese M, Sharma BC, Mostafa I, Bugianesi E, et al. Global perspectives on non-alcoholic fatty liver disease and non-alcoholic steatohepatitis. *Hepatology* 2019;69:2672–82.
- [2] Borrelli A, Bonelli P, Tuccillo FM, Goldfine ID, Evans JL, Buonaguro FM, et al. Role of gut microbiota and oxidative stress in the progression of non-alcoholic fatty liver disease to hepatocarcinoma: current and innovative therapeutic approaches. *Redox Biol* 2018;15:467–79.
- [3] Santhekadur PK, Kumar DP, Sanyal AJ. Preclinical models of non-alcoholic fatty liver disease. *J Hepatol* 2018;68:230–7.
- [4] Fang YL, Chen H, Wang CL, Liang L. Pathogenesis of non-alcoholic fatty liver disease in children and adolescence: from "two hit theory" to "multiple hit model". *World J Gastroenterol* 2018;24:2974–83.
- [5] Adolph TE, Grandner C, Moschen AR, Tilg H. Liver-microbiome axis in health and disease. *Trends Immunol* 2018;39:712–23.
- [6] Takaki A, Kawai D, Yamamoto K. Multiple hits, including oxidative stress, as pathogenesis and treatment target in non-alcoholic steatohepatitis (NASH). *Int J Mol Sci* 2013;14:20704–28.
- [7] Guo S, Nighot M, Al-Sadi R, Alhmodt T, Nighot P, Ma TY. Lipopolysaccharide regulation of intestinal tight junction permeability is mediated by TLR4 signal transduction pathway activation of FAK and MyD88. *J Immunol* 2015;195:4999–5010.
- [8] Chu H, Duan Y, Yang L, Schnabl B. Small metabolites, possible big changes: a microbiota-centered view of non-alcoholic fatty liver disease. *Gut* 2019;68:359–70.
- [9] Kang C, Wang B, Kaliannan K, Wang X, Lang H, Hui S, et al. Gut microbiota mediates the protective effects of dietary capsaicin against chronic low-grade inflammation and associated obesity induced by high-fat diet. *mBio* 2017;8:e417–70.
- [10] Chen M, Hui S, Lang H, Zhou M, Zhang Y, Kang C, et al. SIRT3 deficiency promotes high-fat diet-induced non-alcoholic fatty liver disease in correlation with impaired intestinal permeability through gut microbial dysbiosis. *Mol Nutr Food Res* 2018;e1800612.
- [11] Bird JK, Raederstorff D, Weber P, Steinert RE. Cardiovascular and antiobesity effects of resveratrol mediated through the gut microbiota. *Adv Nutr* 2017;8:839–49.
- [12] Zhao Y, Song W, Wang Z, Wang Z, Jin X, Xu J, et al. Resveratrol attenuates testicular apoptosis in type 1 diabetic mice: role of Akt-mediated Nrf2 activation and p62-dependent Keap1 degradation. *Redox Biol* 2018;14:609–17.
- [13] Bertelli A, Bertelli AA, Gozzini A, Giovannini L. Plasma and tissue resveratrol concentrations and pharmacological activity. *Drugs Exp Clin Res* 1998;24:133–8.
- [14] Walle T, Hsieh F, DeLegge MH, Oatis JJ, Walle UK. High absorption but very low bioavailability of oral resveratrol in humans. *Drug Metab Dispos* 2004;32:1377–82.
- [15] Soleas GJ, Angelini M, Grass L, Diamandis EP, Goldberg DM. Absorption of trans-resveratrol in rats. *Methods Enzymol* 2001;335:145–54.
- [16] Subramanian L, Youssef S, Bhattacharya S, Kenealey J, Polans AS, van Ginkel PR. Resveratrol: challenges in translation to the clinic—a critical discussion. *Clin Cancer Res* 2010;16:5942–8.
- [17] Chen ML, Yi L, Zhang Y, Zhou X, Ran L, Yang J, et al. Resveratrol attenuates trimethylamine-N-oxide (TMAO)-induced atherosclerosis by regulating TMAO synthesis and bile acid metabolism via remodeling of the gut microbiota. *mBio* 2016;7:e2210–5.
- [18] Anhe FF, Roy D, Pilon G, Dufour S, Matamoros S, Varin TV, et al. A polyphenol-rich cranberry extract protects from diet-induced obesity, insulin resistance and intestinal inflammation in association with increased Akkermansia spp. population in the gut microbiota of mice. *Gut* 2015;64:872–83.
- [19] Shin NR, Lee JC, Lee HY, Kim MS, Whon TW, Lee MS, et al. An increase in the Akkermansia spp. population induced by metformin treatment improves glucose homeostasis in diet-induced obese mice. *Gut* 2014;63:727–35.
- [20] Tain YL, Lee WC, Wu K, Leu S, Chan J. Resveratrol prevents the development of hypertension programmed by maternal plus post-weaning high-fructose consumption through modulation of oxidative stress, nutrient-sensing signals, and gut microbiota. *Mol Nutr Food Res* 2018;e1800066.
- [21] Zhao L, Zhang Q, Ma W, Tian F, Shen H, Zhou M. A combination of quercetin and resveratrol reduces obesity in high-fat diet-fed rats by modulation of gut microbiota. *Food Funct* 2017;8:4644–56.
- [22] Anhe FF, Nachbar RT, Varin TV, Vilela V, Dufour S, Pilon G, et al. A polyphenol-rich cranberry extract reverses insulin resistance and hepatic steatosis independently of body weight loss. *Mol Metab* 2017;6:1563–73.
- [23] Carta G, Poddighe L, Serra MP, Boi M, Melis T, Lisai S, et al. Preventive effects of resveratrol on endocannabinoid system and synaptic protein modifications in rat cerebral cortex challenged by bilateral common carotid artery occlusion and reperfusion. *Int J Mol Sci* 2018;19.
- [24] Cani PD, Geurts L, Matamoros S, Plovier H, Duparc T. Glucose metabolism: focus on gut microbiota, the endocannabinoid system and beyond. *Diabetes Metab* 2014;40:246–57.
- [25] Acharya N, Penukonda S, Shcheglova T, Hagymasi AT, Basu S, Srivastava PK. Endocannabinoid system acts as a regulator of immune homeostasis in the gut. *Proc Natl Acad Sci U S A* 2017;114:5005–10.
- [26] Zhang Y, Wang XL, Zhou M, Kang C, Lang HD, Chen MT, et al. Crosstalk between gut microbiota and Sirtuin-3 in colonic inflammation and tumorigenesis. *Exp Mol Med* 2018;50:21.
- [27] Reich CG, Iskander AN, Weiss MS. Cannabinoid modulation of chronic mild stress-induced selective enhancement of trace fear conditioning in adolescent rats. *J Psychopharmacol* 2013;27:947–55.
- [28] Zeng X, Yang J, Hu O, Huang J, Ran L, Chen M, et al. Dihydromyricetin ameliorates nonalcoholic fatty liver disease by improving mitochondrial respiratory capacity and redox homeostasis through modulation of SIRT3 signaling. *Antioxidants Redox Signal* 2019;30:163–83.
- [29] Segata N, Izard J, Waldron L, Gevers D, Miropolsky L, Garrett WS, et al. Metagenomic biomarker discovery and explanation. *Genome Biol* 2011;12:R60.
- [30] Xu J, Lian F, Zhao L, Zhao Y, Chen X, Zhang X, et al. Structural modulation of gut microbiota during alleviation of type 2 diabetes with a Chinese herbal formula. *ISME J* 2015;9:552–62.
- [31] Zhou D, Pan Q, Xin FZ, Zhang RN, He CX, Chen GY, et al. Sodium butyrate attenuates high-fat diet-induced steatohepatitis in mice by improving gut microbiota and gastrointestinal barrier. *World J Gastroenterol* 2017;23:60–75.
- [32] Cani PD, Plovier H, Van Hul M, Geurts L, Delzenne NM, Druart C, et al. Endocannabinoids — at the crossroads between the gut microbiota and host metabolism. *Nat Rev Endocrinol* 2016;12:133–43.
- [33] Pertwee RG, Howlett AC, Abood ME, Alexander SPH, Di Marzo V, Elphick MR, et al. International union of basic and clinical pharmacology. LXXIX. Cannabinoid receptors and their ligands: beyond CB1 and CB2. *Pharmacol Rev* 2010;62:588–631.
- [34] Everard A, Belzer C, Geurts L, Ouwerkerk JP, Druart C, Bindels LB, et al. Cross-talk between Akkermansia muciniphila and intestinal epithelium controls diet-induced obesity. *Proc Natl Acad Sci U S A* 2013;110:9066–71.
- [35] Kelly CJ, Zheng L, Campbell EL, Saeedi B, Scholz CC, Bayless AJ, et al. Crosstalk between microbiota-derived short-chain fatty acids and intestinal epithelial HIF augments tissue barrier function. *Cell Host Microbe* 2015;17:662–71.
- [36] Ploger S, Stumpff F, Penner GB, Schulzke JD, Gabel G, Martens H, et al. Microbial butyrate and its role for barrier function in the gastrointestinal tract. *Ann N Y Acad Sci* 2012;1258:52–9.
- [37] Langille MG, Zaneveld J, Caporaso JG, McDonald D, Knights D, Reyes JA, et al. Predictive functional profiling of microbial communities using 16S rRNA marker gene sequences. *Nat Biotechnol* 2013;31:814–21.